Numerical Simulation of Airflow and Airborne Pathogen Transport in Aircraft Cabins—Part II: Numerical Simulation of Airborne Pathogen Transport

C.-H. Lin, PhD, PE
Member ASHRAE
K.H. Dunn
R.H. Horstman, PE
Member ASHRAE
J.L. Topmiller
M.F. Ahlers
J.S. Bennett, PhD
Associate Member ASHRAE
L.M. Sedgwick, PE
S. Wirogo, PhD

ABSTRACT

There has been considerable public debate regarding airborne disease transmission in the passenger cabin of commercial aircraft. An initial study to develop a numerical tool, using computational fluid dynamics (CFD) methods, for investigating the potential of disease transmission in commercial aircraft, is completed and reported in this paper. To gain insight of the general airflow pattern, a detailed CFD model of a section in the passenger cabin of a B767-300 passenger cabin was built and a Reynolds-averaged Navier-Stokes (RANS) simulation was performed. By comparison with the available test data, the RANS simulation substantially underpredicted the turbulence intensity, especially in and around the breathing zone (Lin et al. 2004). A separate large eddy simulation (LES) was conducted to obtain a more realistic turbulent energy transport in a generic cabin model. The LES-predicted turbulence level is in fairly good agreement with the test data, as reported separately in Lin et al. (2004). Based on the LES results, the k and ε equations used in the RANS simulation were modified by using a special user subroutine. A RANS simulation with adjusted turbulence was then employed to simulate the dispersion of airborne pathogen in the detailed passenger cabin model. These adjustments allow for the simulation of disease transmission using less than 1/100 the computing hardware resources required for an equivalent LES of airflow and particle transport. This paper is an elaboration on the numerical study of the transport of airborne pathogens in an aircraft cabin.

INTRODUCTION

Annually, there are hundreds of millions of passengers that travel using US airlines (Wick and Irvine 1995). The potential for disease transmission in commercial airliners has been reported and studied by many researchers. Moser et al. (1979) reported an outbreak of influenza aboard a B737 jet that was grounded for three hours after an engine failure during a takeoff attempt. Amler et al. (1982) have asserted that certain cases of measles were imported into the US via air travel. McFarland (1993) concluded that the exposure to *M. tuberculosis* might have resulted in transmission during air travel. Based on collected data, Driver et al. (1994) confirmed the transmission of *M. tuberculosis* from one infected flight attendant to others in the same crew. Kenyon et al. (1996) investigated a 1994 incidence of the transmission of tuberculosis by a highly infectious passenger during a long flight. Due to the close proximity of the index patient and other passenger in an aircraft cabin, Wenzel (1996) assessed the potential of airborne transmission using the data from past incidents. Recently, based on the clinical records and after-flight investigations, Olsen et al. (2003) identified the potential transmission pattern of the severe acute respiratory syndrome (SARS) on aircraft.

In a separate paper, Lin et al. (2004) described a process developed using computational fluid dynamics (CFD) to study airplane cabin airflow patterns under the various operating conditions of an aircraft environmental control system (ECS). The objective of this work is to provide a CFD-based methodology to study the potential spread of airborne disease through pathogen dispersion in the passenger cabin of a twin aisle airplane. The B767-300 was chosen as the representative airplane cabin.

The method used focused on the implementation of a commercially available code, with adjustments made to the predicted diffusion to more accurately match test and large

Chao-Hsin Lin, **Raymond H. Horstman**, and **Leigh M. Sedgwick** are associate technical fellows and **Mark F. Ahlers** is a lead engineer at Boeing Commercial Airplanes Group, Seattle, Wash. **Kevin H. Dunn** is an environmental engineer, **Jennifer L. Topmiller** is a mechanical engineer, and **James S. Bennett** is a service fellow at the National Institute for Occupational Safety and Health, Cincinnati, Ohio. **Sutikno Wirogo** is a support engineer at Fluent, Inc., Lebanon, N.H.

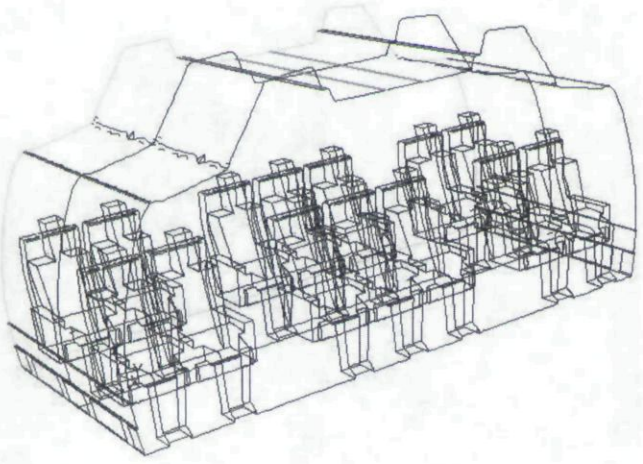

Figure 1 *Two-row B767-300 cabin model (length × width × height = 6.4 × 15.2 × 7.4 ft.*

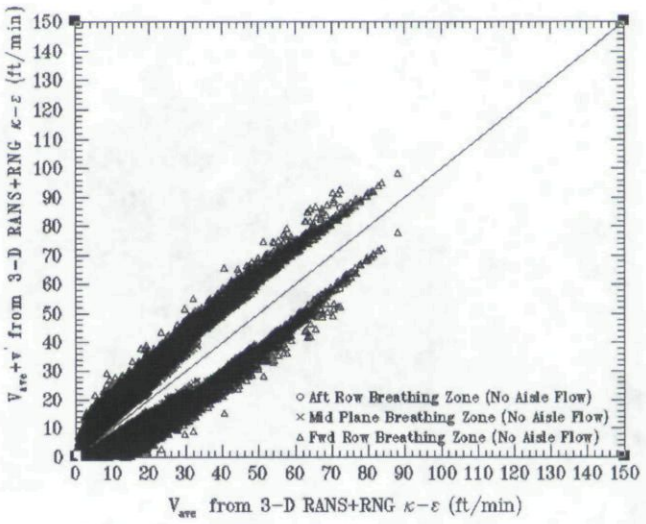

Figure 2 $V_{ave} \pm v'$ *(three-dimensional RANS) vs.* V_{ave} *(three-dimensional RANS) within nominal seated passenger head-height "breathing zone:" no aisle flow case.*

eddy simulation (LES) data, as reported in Lin et al. (2004). The approach, therefore, was to build an average-flow-accurate CFD model for the dispersion of the airborne pathogens and to boost their transport using the more realistic turbulence levels obtained from LES and experimental data. The typical supply diffuser Reynolds number around Re = 3500 lies in the laminar/turbulent transitional zone, making an accurate prediction of the larger scale instabilities difficult. The prediction of the mean velocity of a Reynolds-averaged Navier-Stokes (RANS) simulation with a two-equation turbulence model has, however, been successful to a higher degree. With a proper adjustment to the turbulent diffusion, a RANS should be sufficient to realistically predict the spread of airborne pathogens.

THE RANS AIRFLOW SIMULATION OF A TWO-ROW B767-300 CABIN SECTION

A two-row cabin CFD model was developed for studying disease transmission between neighboring occupants in the lateral and aisle directions on a B767-300 airplane. The model is shown in Figure 1. Note that the model does not include the nozzle geometry due to limitations in the available computing resources. This CFD model, consisting of 4,422,125 tetrahedral cells, is shown in Figure 1. The airflow distribution at the interfaces between the nozzles and the cabin for the B767-300 one-row model was used as an input for the simulation in this two-row model. A FORTRAN program was developed to translate the one-row velocity profile at the interface between the nozzles and the cabin into the two-row configuration. Similarly, a nominal seated passenger head height "breathing zone" in this cabin model was defined with the same dimensions provided earlier.

Two extreme cases, in terms of the ventilation in aircraft cabins, were selected for CFD simulations in this study. The effect of the airflow moving along the FWD-AFT direction of an airplane (called aisle flow) was the criterion for setting up these two cases. These cases are: (1) the no aisle flow case and (2) the "maximum" aisle flow case. For the second case, a FWD-to-AFT aisle flow of 565 SCFM was provided from simulation of air distribution within the entire B767-300 aircraft using a proprietary network code, Joint Engineering Network Analyzer (JENA). JENA also provided the volumetric flow rate exiting each side wall return air grille. Therefore, airflow exiting the cabin normal to each return air grille was specified and a constant outlet flow boundary condition was set at the AFT surface. A 3-D RANS simulation using the renormalization group (RNG) k-ε turbulence model was run for both cases.

As shown in Figure 2, within the "breathing zone," with no aisle flow in the B767-300 cabin, the RANS predicted v' ranges from 3 ft/min to 18 ft/min, which is comparable to that in the simplified cabin with v' ranging from 1 ft/min to 14 ft/min. Therefore, the three-dimensional LES predicted airflow characteristics for the simplified cabin should be applicable to that in the "breathing zone" of the B767-300 cabin. Figures 3 and 5 show the airflow pattern in the center plane "breathing zone" for the no aisle flow case and maximum aisle flow case, respectively. As shown in Figures 2 and 4, the aisle flow seems to retard the velocity fluctuation in those cut planes. This is especially evident on the center plane. Within the "breathing zone," similar results are observed for both the maximum and no aisle flow cases, as shown in Figure 4. Hence, the three-dimensional LES predicted flow characteristics in the "breathing zone" are also applicable to the maximum aisle flow case. Figure 5 shows the airflow pattern on the center plane for the maximum aisle

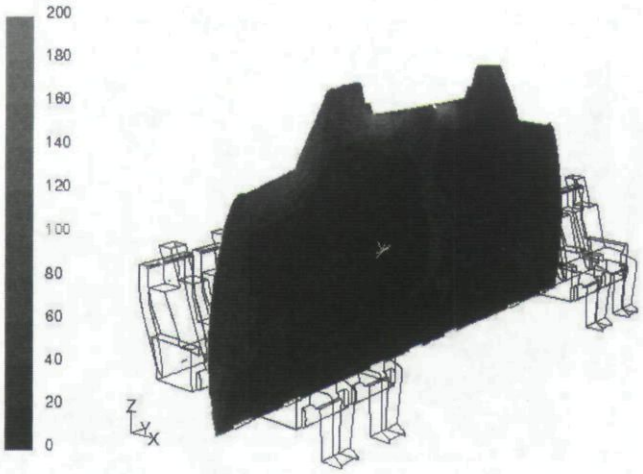

Figure 3 *Airflow pattern at the center plane: no aisle flow case (velocity in ft/min).*

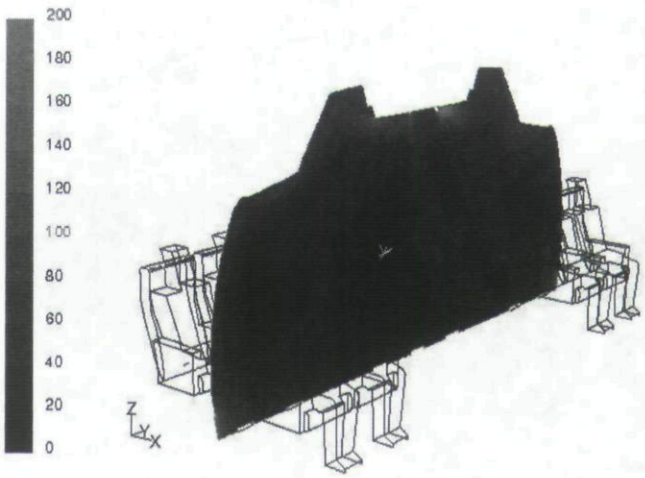

Figure 5 *Airflow pattern at center plane: maximum aisle flow case (velocity in ft/min).*

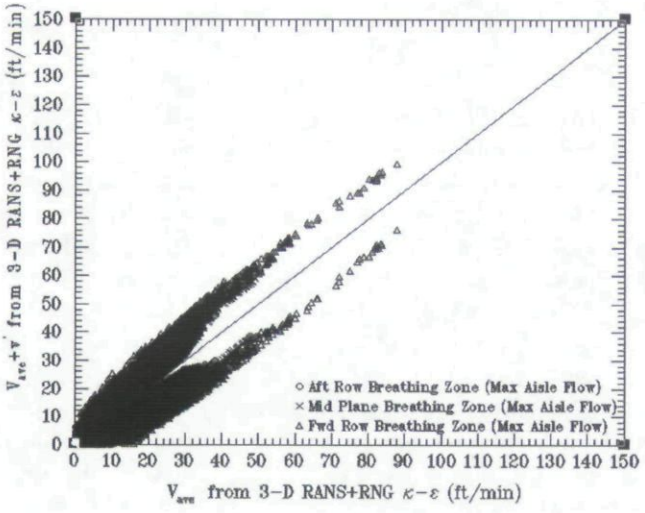

Figure 4 $V_{ave} \pm v'$ *(three-dimensional RANS) vs.* V_{ave} *(three-dimensional RANS) within nominal seated passenger head-height "breathing zone:" maximum aisle flow case.*

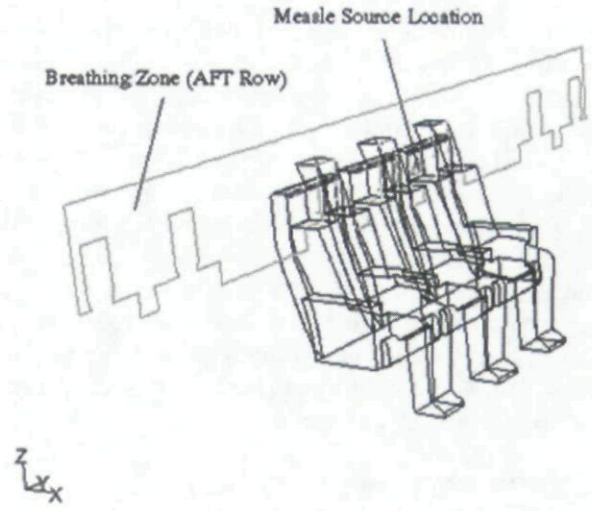

Figure 6 *Location of measles release in cabin.*

flow case. The presence of aisle flow is noticeable in the flow field by comparing that to the no aisle flow case, as shown in Figure 3.

AIRBORNE PATHOGEN DISPERSION SIMULATION IN A B767-300 CABIN SECTION

This section describes a simulation of the dispersion of measles-laden aerosols from a sedentary passenger in an airplane cabin. As shown in Figure 6, the measles release location is placed three inches forward of the mouth area of the middle AFT passenger. The corresponding computational cell at the measles release location is also separated from the fluid zone. The simulation assumes that 100 measles-laden aerosols are released from the passenger within a period of 0.01 seconds. The particle release during the sneeze was modeled using a source term that was manually turned off at $t = 0.01$ seconds into the simulation. Note that the momentum of the released aerosols was not included in this simulation. After the release of measles-laden aerosols, it is assumed that the measles viruses separate from the water during the first 0.01

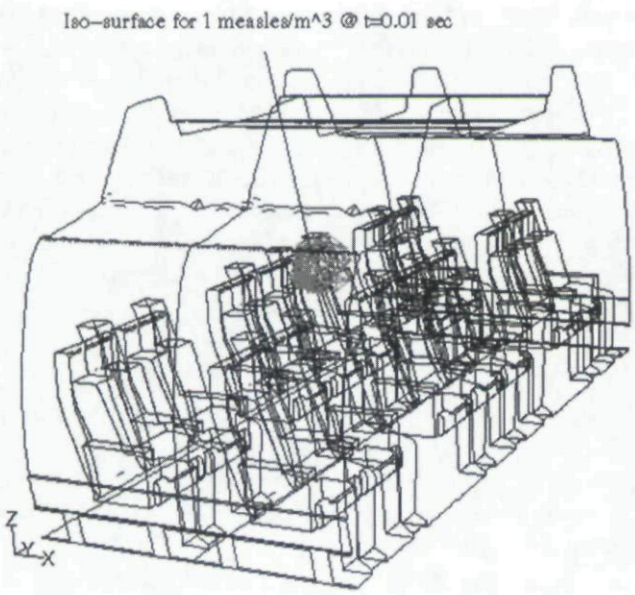

Figure 7 *Iso-surface for 1 measles particle/m^3 at* t = *0.01 seconds after release.*

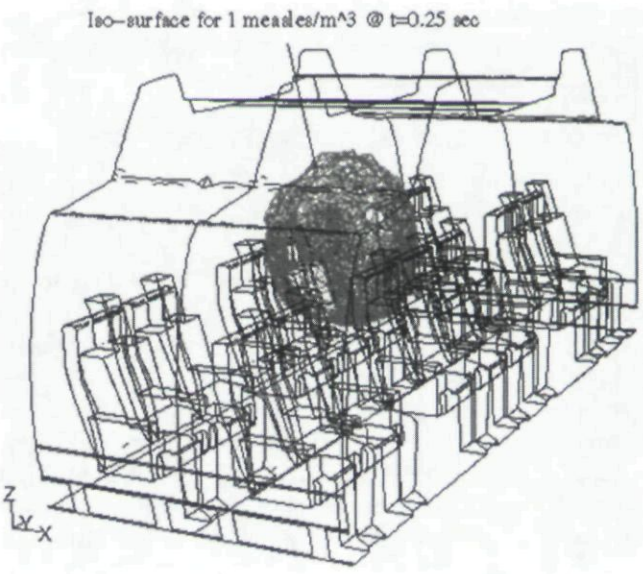

Figure 8 *Iso-surface for 1 measles particle/m^3 at t = 0.25 seconds after release.*

second. The simulation is then resumed with the dispersion of the measles viruses through the cabin section. The simulation also assumes that the measles viruses remaining airborne after the sneeze are small enough to be dispersed by the airflow movement. This assumption allows the flow to be treated as multi-species, which was our approach due to limited computing hardware resources. With no need to track the movement of each aerosol and their interactions with the surrounding fluid, multi-species analysis is significantly less computationally demanding then multiphase analysis.

The aerosol molecular diffusivity and density are assumed to be equal to that of water ($D_v = 2.8 \times 10^{-4}$ ft^2/s, $\rho = 62.4$ lb_m/ft^3). From the three-dimensional LES results, the RANS-derived velocity fluctuations, on average, are about 35.5% of its LES-predicted counterparts. Based on the isotropic assumption used in RANS, the turbulence kinetic energy, k, should be adjusted to be eight times larger than the original values in the flow domain. After reading in the case and data files of the RANS simulation (in here, we used the maximum aisle flow case), a user-defined function, which increases k eight-fold, is created and patched into the original k-field.

Figures 7 through 9 show the results of the measles dispersion simulation. The plots show the iso-surfaces where the concentration of the measles viruses is 1 per m^3 at different points in time. The space enclosed within the iso-surfaces indicates the higher measles number concentrations than the specified value. Conversely, the regions outside of the iso-surfaces means the measles number concentrations are lower that of the specified value.

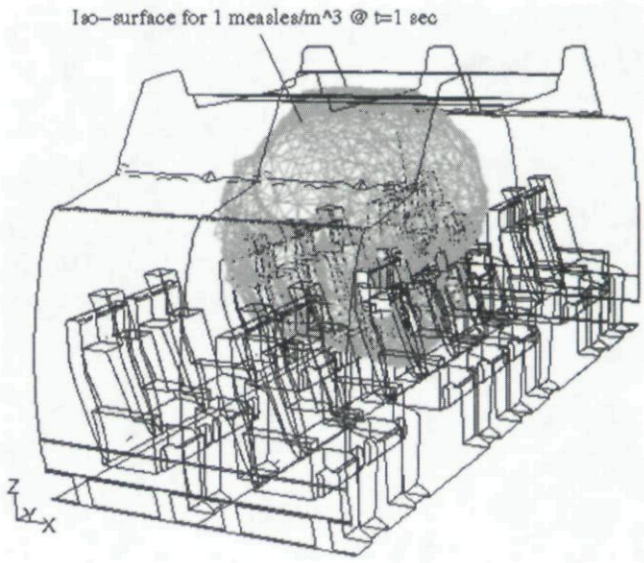

Figure 9 *Iso-surface for 1 measles particle/m^3 at t = 1 second after release.*

The probability of disease transmission as it relates to disease virus concentration is beyond the scope of this study and, therefore, is left for future investigations.

CONCLUSIONS AND RECOMMENDATIONS

In this study, we have explored means to obtain the airflow characteristics using different CFD techniques and, consequently, constructed a procedure to simulate the dispersion of airborne pathogens in an aircraft cabin. Due to the constraints of the available computing resources, simplified cabin models were built to capture the subtlety of the turbulence physics involved in aircraft cabins using LES. We have confirmed the applicability of the LES results to the two-row section of a B767-300 cabin. The LES data obtained in this study also provide the essential airflow information to adjust our RANS simulations and the subsequent particle dispersion simulation for disease transmission. We have demonstrated:

- A viable CFD-based methodology capable of applying the realistically calculated airflow and scalar transport to assess the potential of disease transmission by an airborne pathogen in an aircraft cabin.
- Gas concentration fields can be converted to particle counts using subroutines in commercial CFD software accounting for the sample volume (lungs and breathing rate) to obtain a relative infection probability. (The probability of infection is beyond the scope of this study.)

During the course of this study, several items worthy of further investigation have been identified, which include:

- The effect of aisle flow on the pathogen dispersion in aircraft cabins.
- Simulating the dispersion of disease-laden aerosols in aircraft cabins using the multiphase approach to account for the multiphase effect of aerosols.

ACKNOWLEDGMENTS

The authors are sincerely grateful to Dr. Richard Griffith of Sandia National Laboratories in providing the computing resources for our three-dimensional LES work, and Dr. M.H. Hosni of Kansas State University for his insights into this flow behavior. Within the Boeing Company, we would like to thank our colleague Dr. Ted Wu for verifying our LES results by performing a separate LES using the National Institute of Standards and Technology (NIST) developed Fire Dynamics Simulator (FDS). We are also indebted to Art Davenport and Jeanne Yu for their discussions and support of this work. Lee Briggs, Dean Rogers, and Jim Simek have encouraged and supported the publication of this work.

REFERENCES

Amler, R.W., et al. 1982. Imported measles in the United States. *JAMA*, Vol. 248, pp. 2129-2133.

Driver, C.R., et al. 1994. Transmission of *Mycobacterium tuberculosis* associated with air travel. *JAMA*, Vol. 272, pp. 1031-1035.

Kenyon, T.A., et al. 1996. Transmission of multidrug-resistant *Mycobacterium tuberculosis* during a long airplane flight. *The New England J. of Medicine* 334(15):933-938.

Lin, C.H., et al. 2004. Numerical simulation of airflow and airborne pathogen transport in aircraft cabins: Part I: Numerical simulation of the flow field (submitted to ASHRAE for publication).

McFarland, J.W. 1993. Exposure to *Mycobacterium tuberculosis* during air travel. *The Lancet*, Vol. 342, pp. 112-113.

Moser, M.R., et al. 1979. An outbreak of influenza aboard a commercial airliner. *American J. of Epidemiology* 110(1):1-6.

Olsen, S.J., et al. 2003. Transmission of the severe acute respiratory syndrome on aircraft. *The New England J. of Medicine* 349(25):2416-2422.

Wenzel, R.P. 1996. Airline travel and infection. *The New England J. of Medicine* 334(15):981-982.

Wick, R.L., Jr., and L.A. Irvine. 1995. The microbiological composition of airliner cabin air. *Aviation, Space, and Environmental Medicine*, Vol. 66, pp. 220-224.